Opto-Electronic Engineering

Article

2017, Vol 44, Issue 4

Functional micro-concrete 3D hybrid structures fabricated by two-photon polymerization

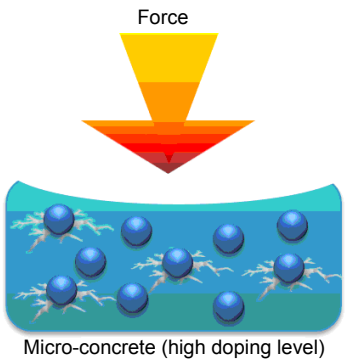

Yang Li[1,2†], Lianwei Chen[1†], Fang Kong[3], Zuyong Wang[1], Ming Dao[3], Chwee Teck Lim[3], Fengping Li[4] and Minghui Hong[1*]

[1]National University of Singapore, 4 Engineering Drive 3, Singapore 117576, Singapore; [2]State Key Laboratory of Optical Technologies for Nano-Fabrication and Micro-Engineering, Institute of Optics and Electronics, Chinese Academy of Sciences, Chengdu 610209, China; [3]Singapore MIT Alliance Research and Technology, Singapore 138602, Singapore; [4]College of Mechanical and Electrical Engineering, Wenzhou University, Wenzhou 325025, China.

Abstract: Arbitrary micro-scale three-dimensional (3D) structures fabrication is a dream to achieve many exciting goals that have been pursued for a long time. Among all these applications, the direct 3D printing to fabricate human organs and integrated photonic circuits are extraordinary attractive as they can promote the current technology to a new level. Among all the 3D printing methods available, two-photon polymerization (2PP) is very competitive as it is the unique method to achieve sub-micron resolution to make any desired tiny structures. For the conventional 2PP, the building block is the photoresist. However, the requirement for the building block is different for different purposes. It is very necessary to investigate and improve the photoresist properties according to different requirements. In this paper, we presented one hybrid method to modify the mechanical strength and light trapping efficiency of the photoresist, which transfers the photoresist into the micro-concretes. The micro-concrete structure can achieve ±22% strength modification via a silica nano-particles doping. The structures doped with gold nano-particles show tunable plasmonic absorption. Dye doped hybrid structure shows great potential to fabricate 3D micro-chip laser.

Keywords: 3D nano-printing; two-photon polymerization; hybrid; micro-concrete

DOI: 10.3969/j.issn.1003-501X.2017.04.002 **Citation:** *Opto-Elec Eng*, 2017, **44**(4): 393−399

1 Introduction

Two-photon polymerization (2PP) is a 3D fabrication technique that has long fascinated the researchers: its resolution is not limited by diffraction limit and it is able to realize true 3D structure in micro-scale. These unique features cannot be matched by other 3D printing methods [1-3]. The most impressive feature of the 2PP is its capability to fabricate sub-micron scales 3D structure of arbitrary shapes. To achieve it, 2PP relies on the direct laser writing to transfer the pattern into the photoresist material by the two photon absorption to initialize the in-situ polymerization. Based on this principle, 2PP offers resolution down to 100 nm and is free of high temperature annealing or laser fusion processes.

Even though 2PP has many superior properties, it is often considered as a supporting role to make the initial polymer structural molds or backbones for further processing steps [4-6]. The reason is that the photoresist used in 2PP lacks the proper material properties to act as the functional material in different applications. It remains an important question whether we can further improve the photoresist and realize the required functionalities to truly improve the feasibility of 2PP technique. It is very promising if 2PP can directly construct the human organs, photonic circuits and other important applications [7-11]. To realize it, it is a key to study how to make the photo-resist controllable according to different demands.

In this paper, we proposed one hybrid method to directly make arbitrary micro-structures with desired functionalities. We have also demonstrated that this new hybrid method can maintain the existing good features of the 2PP method while upgrades its functionality to a higher level by making a large scale pattern with fine

Received 24 November 2016; accepted 12 January 2017
† These authors contributed equally to this work.
* E-mail: elehmh@nus.edu.sg

features. Compared with other lithographic technologies, our approach is more favorable since the fabrication is fast hence it is more suitable for scalable production. Specifically, the 2PP process is adapted to directly process three hybrid composites with different functionalities: 1) Mechanical functional materials: micro-concrete with tunable mechanical strength for bio-structure construction; Photonic functional materials: 2) plasmonic absorbers to be used in light trapping sensors and 3) photonic light sources with highly customized designs. These three specific works serve as good examples to demonstrate that the hybrid 2PP method can be introduced as a unique and powerful 3D nano-printing technique for massive scale effective fabrication to make the key functional components for various applications.

2 Fabrication principles

To improve the material property of the photoresist, our approach is to hybrid the functional components with the photoresist. After the hybridization, the next step is a typical coating and exposure process for 2PP as shown in Fig. 1. Then, the sample is sent to be developed to remove the unexposed photoresist. Finally, isopropanol (IPA) and deionized (DI) water are used to clean the sample from the remaining chemicals. In this process, two most important processing parameters are laser power and scanning speed in the exposure process, which greatly affects the geometry of the 3D structures. Laser power is adjusted by a variable attenuator while the scanning speed is controlled by the nano-stage movement. For each type of functional material, different parameters have been tested for the photo-exposure. The smallest size of the 2PP structure achieved is ~120 nm as shown in our experiment, which cannot be achieved with other conventional 3D printing techniques [12, 13]. In this work, three approaches are tested: a) biocompatible materials with tunable mechanical properties (Fig. 2), b) hybrid optical material for integrated photonics (Fig. 3), and c) micro photonic light source (Fig. 4). The details for the material preparation are summarized in the method section. Fig. 4(a) shows that the 2PP technique can be used for the fabrication of a woodpile hybrid structure. The lines are continuous and smooth. The line width of such structure is around 500 nm to prevent the collapse when the pattern is repeated over a large area. Clearly, the doping of nano-particles does not affect the fabrication of multi-layer structures. Hence, doping nanoparticles in photoresist does not affect the photochemical property of

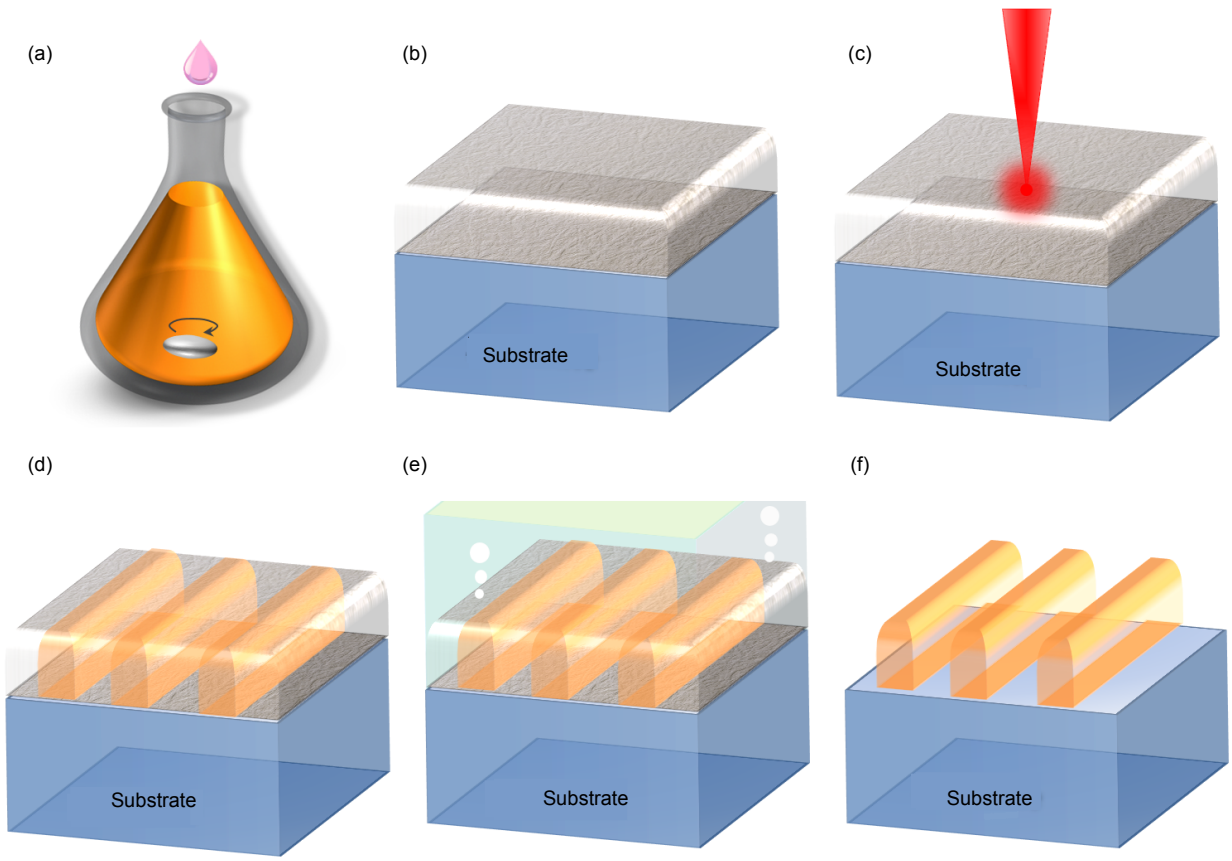

Fig. 1 Process flow of two-photon polymerization. (a) Photoresist preparation. (b) Photoresist coating. (c) Laser exposure. (d) Pre-develop treatment. (e) Photoresist develop. (f) Post-develop treatment.

photoresist.

3 Biocompatible materials with tunable mechanical properties

3D customized biological structures printing has great impact on the fabrication of artificial human prosthesis and reliable testing ground for medical researches. The current 3D printing techniques can only achieve the resolution more than 10 μm, while the capillaries in the human body have the diameter less than 8 μm [14]. These fine structures are extremely important for the functionalities of the human organs. 2PP fabrication can meet all these requirements with its highly customized 3D fabrication scheme, sub-micron resolution, bio-compatible building materials, simple procedure and reasonably fast speed. The bio-systems consist of soft materials as well as hard materials [15]. For instance, the common structural proteins and elastins in the human blood vessels have the Young's modulus of more than 50% with the maximum of 1 MPa [16]. This complexity requires the 2PP functional materials to have tunable mechanical properties in order to satisfy various purposes.

To achieve this aim, the porous silica nano-particles are mixed with the photoresist at different concentrations (Type A: no dopants; Type B, C, D, E are doped with silica nano-particles at a concentration of 0.6×10^{13} cm^{-3}, 1.2×10^{13} cm^{-3}, 1.8×10^{13} cm^{-3} and 2.4×10^{13} cm^{-3}, respectively). Details for the fabrication are summarized in the method section. The Young's modulus is measured by an atomic force microscope (AFM, NanoWizard 2, JPK Instruments) via the contact mode. The deformation vs.

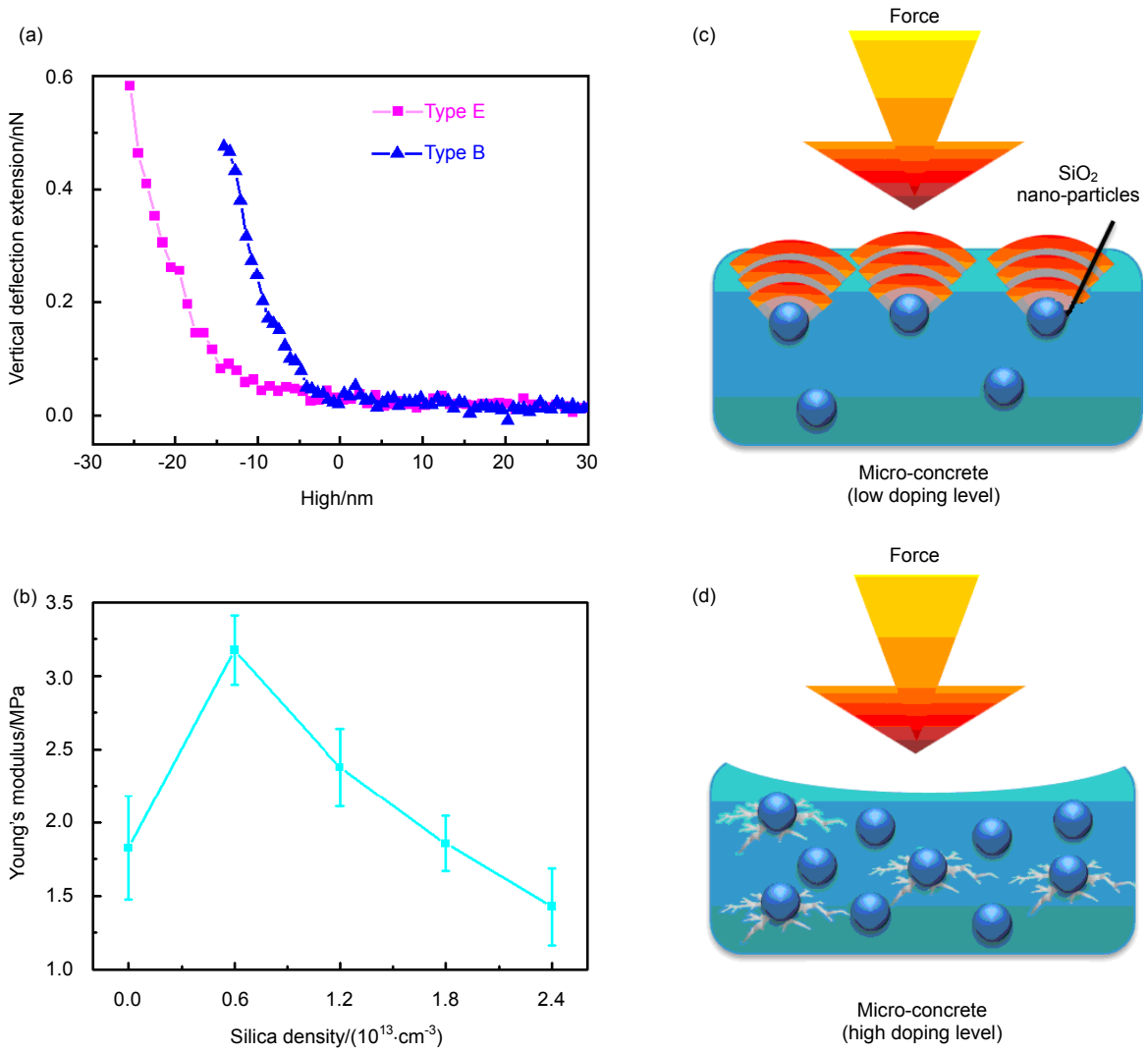

Fig. 2 (a) AFM contact mode results for the mechanical property measurement. (b) Young's modulus values measured from 2PP microstructures fabricated from non-doped and doped photoresists. Type A: no dopants; Type B, C, D, E are doped with silica nano-particles at a concentration of 0.6×10^{13} cm^{-3}, 1.2×10^{13} cm^{-3}, 1.8×10^{13} cm^{-3} and 2.4×10^{13} cm^{-3}, respectively. Mechanical behaviors of the micro-concretes when doped with (c) low and (d) high concentrations of silica nano-particles.

force curves are measured by a quadratic pyramidal tip. Two typical curves for Type B and Type E are shown in Fig. 2(a). Spherical Hertz model is used to fit the data and the Young's modulus can be calculated with the following equation [17]:

$$\boldsymbol{F} = \frac{1}{2^{1/2}} \frac{E \tan\theta}{1-\nu} \delta^2 , \quad (1)$$

where $\boldsymbol{F}$ is the total force (vertical deflection), E the Young's modulus, δ the indentation depth, ν Poisson's ratio, and θ nominal semi-included angle of pyramidal tip.

The results are presented in Fig. 2(b). It is obvious that the Young's modulus is dependent on the density of the silica nano-particles. At the moderate level of silica doping density (0.6×10^{13} cm^{-3}), the Young's modulus increases by 70% compared to the reference without any dopants. However, when the doping concentration is further increased to 2.4×10^{13} cm^{-3}, it is interesting to observe that the Young's modulus of the sample decreases monotonously.

It should be noted that the doping concentration is quite small (3.2% by weight for Type E). Even at this low doping concentration, a notable variation of more than ±22% can be achieved. After the laser exposure, these silica nano-particles serve dual purposes in the hybrid systems, which are illustrated in Figs. 2(c) and 2(d). The Young's modulus of silica is more than 70 GPa (3 orders higher than the 2PP photoresist) [18]. For the first case, such silica nano-particles are like the "hard stones" in the concrete. When the doping concentration is small, these "hard stones" inside the photoresist demonstrate the similar functionality as the reinforcements inside the concretes. Introduction of such nanoparticles consequently increases the overall Young's modulus of the micro-concrete. In the second case, these external components are also defects in the polymer matrix. An excess doping of such nano-particles affects the binding of the polymer chains and weakens the structure [19]. In addition, nanoparticles tend to agglomerate at a higher concentration. Particles' agglomeration flaws the material's surface, which restrains stress movement and hence reduces the mechanical strength[20]. As a result, the Young's modulus of the hybrid material decreases.

4 Hybrid optical material for integrated photonics

The hybrid fs-laser 2PP fabrication method also has great potentials in the photonic applications [21-29]. How to trap the light efficiently is the general issue for most types of the light sensors which are the most fundamental elements in the modern optics. For instance, the surface enhanced Raman spectroscopy utilizes the surface plasmon resonance effect to enhance the collection of the Raman signals. It is important for the sensitivity of the light sensors, the performance of charge-coupled devices, and the functionality of spectroscopy techniques.

Nanostructures with the gold nanoparticles are fabricated by 2PP as shown in Fig. 3(a). To characterize the tunability of the light trapping properties, the transmittance of the hybrid fs-laser 2PP samples (doped with gold nano-particles of 10 nm for sample A and 30 nm for sample B) are measured from 400 nm to 900 nm, which corresponds to the absorption peaks of different gold nano-particles in photoresist. As the results are shown in Fig. 3(b), the samples doped with the gold nano-particles demonstrate absorption peaks at different wavelengths (616 nm for the 10 nm gold nanoparticles and 651 nm for the 30 nm gold nanoparticles), which shows the capability that its absorption features can be tuned via doping plasmonic nano-particles with different sizes. It is worth to mention that the sample is very thin (less than 5 μm). The light trapping can be further improved with a thicker sample. These two transmittance drops corresponding to the surface plasmon resonances of the gold nano-particles. Such surface plasmon resonance is due to the oscillation of the electrons at the surface of the gold nano-particles. Hence, the resonance mode is dependent on the area of the surface and the change of the particle size affects the resonance peak intensity greatly.

Photonic components based on the surface plasmon have many unique features that are widely used in the functional devices. To better trap the light, these structures mostly favor high spatial configurations and highly customized designs for different signal types. 2PP process is more suitable than other fabrication methods to make these plasmonic structures due to its fast speed and excellent flexibility for the 3D structures' fabrication. The micro-concrete doped with the gold nano-particles enhances the conventional fs-laser 2PP method into a new fabrication technique that can make optical sensors based on functional plasmonic materials.

5 Micro-photonic light source

The 2PP technique has been proven to be capable of writing optical waveguides with a mechanically flexible polymer structure [30]. Direct laser writing in the 2PP process allows the fabrication of arbitrary and complex 3D structures. Meanwhile, our study shows that the doping of Rhodamine 6G (R6G) has no significant effect on the 2PP process. Therefore, 2PP is a suitable method for fabricating 3D hybrid light emission sources in integrated photonic circuits.

To investigate the optical properties of the hybrid structures, we fabricated the R6G doped hybrid structures of a fishnet pattern with an area of 0.5 mm×0.5 mm (Fig. 4(a)). To improve its performance, the fabricated lines need to be continuous and uniform. Furthermore, the surface needs to be smooth and defect free to minimize optical loss. Hence, we optimized the scanning speed (1 mm/s) and scanning step (3 μm) to improve the uniformity of the line and the smoothness of the surface.

DOI: 10.3969/j.issn.1003-501X.2017.04.002

Another waveguide is also fabricated on the hybrid sample to offer a direct view of this light emission effect. Then, the 532 nm laser light from the laser diode is coupled into one side of the R6G doped hybrid waveguide with the output power of 40 mW. As can be seen from the optical image in Fig. 4(b), the light source emits strong orange light which is the combination of the green excitation light and the yellow fluorescent light. The light is uniformly distributed throughout the light source, indicating a low optical loss. Since the waveguide has low optical loss and strong fluorescent emission, it can be used as the light source for a micro-fiber laser. This micro-fiber laser needs a resonator which consists of Bragg gratings at the two ends of the fiber. This potential application will be investigated in our future study to make micro/nano-laser sources. Fig. 4(c) shows the fluorescence spectrum of the hybrid structure. During the propagation of the 532 nm laser light along the core of

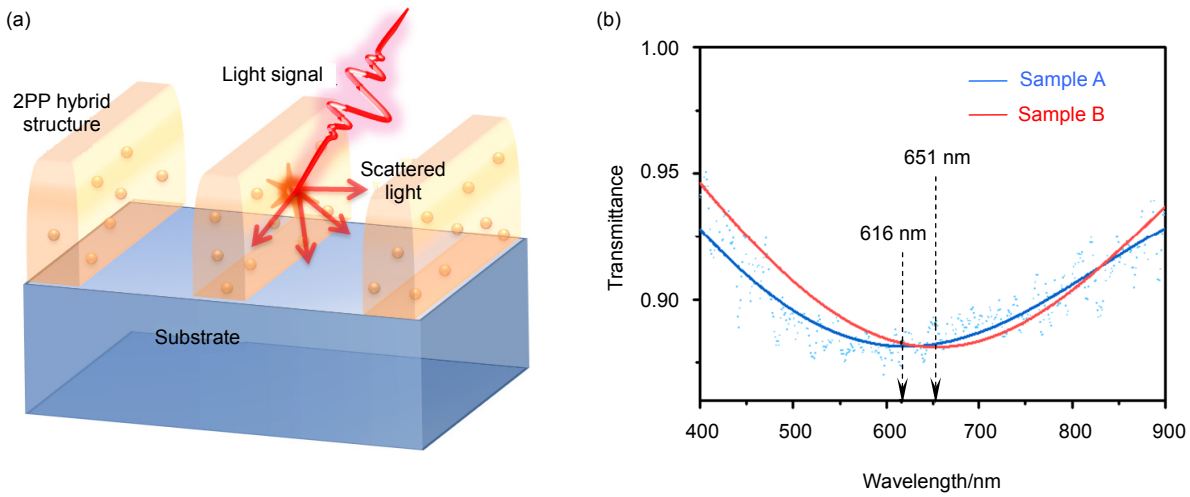

Fig. 3 (a) Schematic diagram of light trapping structure doped with gold nano-particles. (b) Transmittance spectra of the samples doped with gold nano-particles at various sizes.

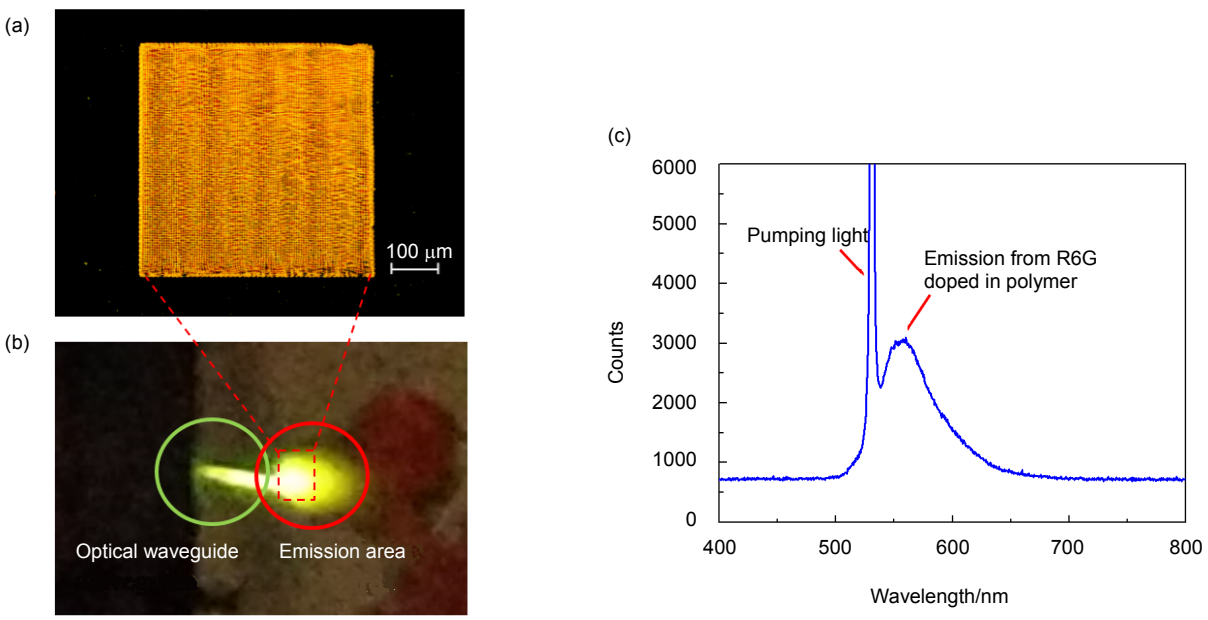

Fig. 4 (a) Optical image of fishnet structure. (b) Optical image of the light emission material pumped with a 532 nm laser. (c) Emission spectrum of the light emission source doped with R6G.

the hybrid light source, a strong fluorescent emission peaked at 560 nm is detected. This value is in good agreement with the ones reported in the literature for R6G [31]. It indicates that the R6G dyes are not damaged or degraded during the 2PP fabrication process.

6 Conclusions

In summary, a new hybrid 2PP fabrication method is demonstrated in this work. Via doping different nano-particles, the fs-laser 2PP photoresist is transferred into the micro-concretes that possess different novel functionalities. Photoresist doped with the porous silica nano-particles demonstrates tunable mechanical strength of ±22%, which makes it feasible to nano-engineer tiny and crucial biological structures. Furthermore, doping the gold nano-particles into the photoresist also shows tunable light trapping features. By varying the sizes of the gold nano-particles, the absorption features can be tuned, which is flexible to meet the requirements of different photonic sensors. These results reveal the potentials of the 2PP method as the functional materials for various applications. It should be noted that there are wide choices of the materials available that can be further explored as the potential dopant choices for micro-concretes, such as carbon nano-tubes and other metallic particles. There is plenty of space to further improve the functionality of such micro-concretes.

7 Methods

7.1 Materials preparation

Two types of the functional materials are hybridized into the 2PP photoresist (IP-Dip, Nanoscribe) to investigate their effects in transforming the 2PP photoresist into the functional micro-concretes. The methods are summarized as follows:

7.1.1 Bio-compatible micro-concrete with mesoporous bioactive silica nano-particles

Silica nano-particles are first added into IPA at a concentration of 15 mg/ml and then sonicated for 20 minutes to form a uniform nanoparticle colloid. A mixture of silica nano-particles and 2PP photoresist is prepared by direct mixing of these two materials at a volume ratio of 1:1 and stirring for 10 minutes.

Transparent cover glass is used as the substrate. The glass is sonicated in each liquid for 10 minutes: deionized (DI) water, acetone, and DI water. The silica nano-particle/2PP photoresist mixture is drop-coated on the silica substrate. The mixture is then baked at 60℃ for 20 minutes in order to evaporate the IPA solvent.

7.1.2 Plasmonic light trapper with gold nano-particles

The hybrid procedure for gold nano-particles (Nanocs, 0.1% in aqueous solution) is different from the method to mix the silica porous nano-particles. It is because of the insolubility between the water and the photoresist. 20 μl gold nano-particles colloid is drop-coated on the glass substrate and then baked at 60 ℃ until the colloid is concentrated. Then 20 μl photoresist is added into the gold nano-particles. The gold nano-particles have the diameters of 10 nm and 30 nm. The mixture is stirred for 20 minutes to ensure uniform distribution of the gold nano-particles in the photoresist.

7.1.3 Hybrid light emission source

R6G (Sigma-Aldrich) is first dissolved in IPA at a concentration of 15 mg/ml. A mixture of R6G and 2PP photoresist is prepared by the direct mixing of these two materials at a volume ratio of 1:1 and stirring for 20 minutes. After cleaning the glass substrate, the mixture is drop coated on the substrate via the same methods mentioned previously.

7.2 2PP processing

In this work, a near-infrared Ti:sapphire femtosecond laser beam (50 fs-pulse width, 80 MHz repetition rate, 800 nm central wavelength, Coherent) is used to fabricate 3D hybrid structures. The process flow is shown in Fig. 1. A high numerical aperture (NA) objective lens is used to focus the fs-laser beam into the hybrid photoresist on the glass substrate. The sample is placed on a 6-axis motorized nano-stage (XY-Tripod-Theta 6 Axis System, Alio Industries). The laser system and nano-stage are controlled by customized software (CyberLase, IDI laser). The pattern designs, such as fishnet and woodpile structures, are drawn by this software. The exposure dose is controlled by the laser power and the moving speed of the nano-stage. To obtain the smallest feature size, it is found that the optimized average laser power and scanning speed are 8.4 mW and 30 μm/s, respectively by an oil immersion objective lens (NA = 1.4, 100×). In order to increase the aspect ratio for the fabrication of large-size pattern, another objective lens operating in air (NA = 0.9, 100×) is also used to fabricate the 3D hybrid structures at the laser power of 270 mW and scanning speed of 5 mm/s. After the laser exposure is completed, the sample is first immersed in propylene glycol monomethyl ether acetate (PGMEA) for 30 minutes followed by immersion in an IPA solution for 10 minutes to remove unpolymerized photoresist. Thus, only the polymerized photoresist is left on the substrate. Then the sample is analyzed under an optical microscope and scanning electron microscope (SEM) and used for further characterizations.

Acknowledgements

The authors would like to thank Prof. Thian Eng San and Dr. Wang Dong for providing the silica nano-particles used in experiment. This work is financially supported by A*STAR, SERC 2014 Public Sector Research Funding (PSF) (Grant: SERC Project, 1421200080), 973 Program of China (2013CBA01700) and Chinese Nature Science Grant (61675207, U1609209). Kong Fang and Dao Ming acknowledge the support by the National Research

Foundation Singapore through Singapore-MIT Alliance for Research and Technology (SMART) Infectious Disease IRG research programme. Li Yang acknowledges the support from China Scholarship Council (CSC).

References

1 Mironov V, Boland T, Trusk T, *et al*. Organ printing: computer-aided jet-based 3D tissue engineering[J]. *Trends in Biotechnology*, 2003, **21**(4): 157–161.

2 Seitz H, Rieder W, Irsen S, *et al*. Three-dimensional printing of porous ceramic scaffolds for bone tissue engineering[J]. *Journal of Biomedical Materials Research Part B: Applied Biomaterials*, 2005, **74B**(2): 782–788.

3 Giordano R A, Wu B M, Borland S W, *et al*. Mechanical properties of dense polylactic acid structures fabricated by three dimensional printing[J]. *Journal of Biomaterials Science, Polymer Edition,* 1997, **8**(1): 63–75.

4 Zhou Wenhui, Kuebler S M, Braun K L, *et al*. An efficient two-photon-generated photoacid applied to positive-tone 3d microfabrication[J]. *Science*, 2002, **296**(5570): 1106–1109.

5 Cumpston B H, Ananthavel S P, Barlow S, *et al*. Two-photon polymerization initiators for three-dimensional optical data storage and microfabrication[J]. *Nature*, 1999, **398**(6722): 51–54.

6 Serbin J, Ovsianikov A, Chichkov B. Fabrication of woodpile structures by two-photon polymerization and investigation of their optical properties[J]. *Optics Express,* 2004, **12**(21): 5221–5228.

7 Serbin J, Egbert A, Ostendorf A, *et al*. Femtosecond laser-induced two-photon polymerization of inorganic-organic hybrid materials for applications in photonics[J]. *Optics Letters,* 2003, **28**(5): 301–303.

8 Peltola S M, Melchels F P W, Grijpma D W, *et al*. A review of rapid prototyping techniques for tissue engineering purposes[J]. *Annals of Medicine,* 2008, **40**(4): 268–280.

9 Ma H, Jen A K Y, Dalton L R. Polymer-based optical waveguides: Materials, processing, and devices[J]. *Advanced Materials,* 2002, **14**(19): 1339–1365.

10 Luo Xiangang. Principles of electromagnetic waves in metasurfaces[J]. *Science China Physics, Mechanics & Astronomy*, 2015, **58**(9): 594201.

11 Luo Xiangang, Pu Mingbo, Ma Xiaoliang, *et al*. Taming the electromagnetic boundaries via metasurfaces: from theory and fabrication to functional devices[J]. *International Journal of Antennas and Propagation*, 2015, **2015**: 204127.

12 Raymo F M. Digital processing and communication with molecular switches[J]. *Advanced Materials,* 2002, **14**(6): 401–414.

13 Zhang Xian, Yu Xiaoqiang, Sun Yuming, *et al*. Synthesis, structure and nonlinear optical properties of two new one and two-branch two-photon polymerization initiators[J]. *Chemical Physics*, 2006, **328**(1-3): 103–110.

14 Hoffman G S, Weyand C M, Langford C A, *et al*. Inflammatory diseases of blood vessels[M]. Oxford: Wiley-Blackwell, 2012.

15 Taylor J J, Memmler R L, Cohen B J. Memmler's structure and function of the human body[M]. Philadelphia: Lippincott Williams & Wilkins, 2005.

16 Wuyts F L, Vanhuyse V J, Langewouters G J, *et al*. Elastic properties of human aortas in relation to age and atherosclerosis: a structural model[J]. *Physics in Medicine and Biology*, 1995, **40**(10): 1577–1597.

17 Rico F, Roca-Cusachs P, Gavara N, *et al*. Probing mechanical properties of living cells by atomic force microscopy with blunted pyramidal cantilever tips[J]. *Physical Review E*, 2005, **72**(2): 021914.

18 Wachtman J B, Cannon W R, Matthewson M J. Mechanical properties of ceramics[M]. 2nd ed. Hoboken, NJ: John Wiley & Sons, 2009.

19 Quaresimin M, Bertani R, Zappalorto M, *et al*. Multifunctional polymer nanocomposites with enhanced mechanical and anti-microbial properties[J]. *Composites Part B*, 2015, **80**: 108–115.

20 Zhang Qingxin, Yu Zhongzhen, Xie Xiaolin, *et al*. Crystallization and impact energy of polypropylene/$CaCO_3$ nanocomposites with nonionic modifier[J]. *Polymer*, 2004, **45**(17): 5985–5994.

21 Huo Qisheng, Zhao Dongyuan, Feng Jianglin, *et al*. Room temperature growth of mesoporous silica fibers: a new high-surface-area optical waveguide[J]. *Advanced Materials*, 1997, **9**(12): 974–978.

22 Chen Lianwei, Zheng Xiaorui, Du Zheren, *et al*. A frozen matrix hybrid optical nonlinear system enhanced by a particle lens[J]. *Nanoscale,* 2015, **7**(36): 14982–14988.

23 Zhou Y, Chen L W, Du Z R, *et al*. Tunable optical nonlinearity of silicon nanoparticles in solid state organic matrix[J]. *Optical Materials Express*, 2015, **5**(7): 1606–1612.

24 Pu Mingbo, Li Xiong, Ma Xiaoliang, *et al*. Catenary optics for achromatic generation of perfect optical angular momentum[J]. *Science Advances*, 2015, **1**(9): e1500396.

25 Li Xiong, Pu Mingbo, Zhao Zeyu, *et al*. Catenary nanostructures as compact Bessel beam generators[J]. *Scientific Reports*, 2016, **6**: 20524.

26 Luo Xiangang, Ishihara T. Surface plasmon resonant interference nanolithography technique[J]. *Applied Physics Letters,* 2004, **84**(23): 4780–4782.

27 Feng Qin, Pu Mingbo, Hu Chenggang, *et al*. Engineering the dispersion of metamaterial surface for broadband infrared absorption[J]. *Optics Letters*, 2012, **37**(11): 2133–2135.

28 Pu Mingbo, Zhao Zeyu, Wang Yanqin, *et al*. Spatially and spectrally engineered spin-orbit interaction for achromatic virtual shaping[J]. *Scientific Reports*, 2015, **5**: 9822.

29 Luo Xiangang, Yan Lianshan. Surface plasmon polaritons and its applications[J]. *IEEE Photonics Journal,* 2012, **4**(2): 590–595.

30 Infuehr R, Pucher N, Heller C, *et al*. Functional polymers by two-photon 3D lithography[J]. *Applied Surface Science,* 2007, **254**(4): 836–840.

31 Parker S T, Domachuk P, Amsden J, *et al*. Biocompatible silk printed optical waveguides[J]. *Advanced Materials*, 2009, **21**(23): 2411–2415.